Current-driven magnetic rearrangements in spin-polarized point contacts

Maria Stamenova and Stefano Sanvito*
School of Physics, Trinity College, Dublin 2, Ireland

Tchavdar N. Todorov
School of Mathematics and Physics, Queen's University of Belfast, Belfast BT7 INN, United Kingdom
(Received 5 May 2005; published 6 October 2005)

A method for investigating the dynamics of atomic magnetic moments in current-carrying magnetic point contacts under bias is presented. This combines the nonequilibrium Green's function (NEGF) method for evaluating the current and the charge density with a description of the dynamics of the magnetization in terms of quasistatic thermally activated transitions between stationary configurations. This method is then implemented in a tight-binding (TB) model with parameters chosen to simulate the main features of the electronic structures of magnetic transition metals. We investigate the domain wall (DW) migration in magnetic monoatomic chains sandwiched between magnetic leads, and for realistic parameters find that collinear arrangement of the magnetic moments of the chain is always favorable. Several stationary magnetic configurations are identified, corresponding to a different number of Bloch walls in the chain and to a different current. The relative stability of these configurations depends on the geometrical details of the junction and on the bias; however, we predict transitions between different configurations with activation barriers of the order of a few tens of meV. Since different magnetic configurations are associated with different resistances, this suggests an intrinsic random telegraph noise at microwave frequencies in the *I-V* curves of magnetic atomic point contacts at room temperature. Finally, we investigate whether or not current-induced torques are conservative.

DOI: 10.1103/PhysRevB.72.134407 PACS number(s): 75.75.+a, 73.63.Rt, 75.60.Jk, 72.70.+m

I. INTRODUCTION

Most of the intriguing properties of ferromagnetic nanoscale atomic structures arise from the close interplay between magnetic phenomena and electronic transport. As the magnetization can be controlled on a length scale smaller than the spin-diffusion length of the conduction electrons,[1] the spin scattering is affecting the overall resistance of an atomic ferromagnetic device. This is the principle behind the giant magnetoresistance effect (GMR).[2,3] Remarkably, the opposite effect is also possible, i.e., the electronic current, as proposed by Slonczewski,[4] can *transfer spin* and alter the magnetic configuration of the underlying ferromagnetic structure. Magnetization switching, caused by spin-polarized currents, has been observed experimentally in point contact measurements[5,6] and in nanopillars.[7]

It is clear that the modeling of these atomic-scale ferromagnetic devices requires the combined description of electronic transport and of the magnetization dynamics at the atomic level. For this purpose we have developed a general scheme for evaluating spin-polarized currents and associated current-induced torques, which allows us to investigate the magnetization dynamics and the transport of magnetic point contacts under bias. Our problem and our method mimic closely, in philosophy, electromigration problems (thermally activated current-driven structural rearrangements), where now the direction of the local magnetic moments takes the place of the atomic positions as "reaction coordinate."

Although our scheme is general and is conceptually transferable to first-principles Hamiltonians (for instance, within density functional theory), here we apply the method to a simple self-consistent tight-binding (TB) model. This has the benefit of being reasonably realistic while keeping the computational overheads to a minimum.

The paper is organized as follows: in Secs. II A and II B we introduce our method, describe the model, and sketch out the techniques used for the calculations. Then, in Sec. II C, we discuss our approach to the interplay between spin-polarized transport and the magnetic configuration, applied to a particular atomic structure. In Sec. III we report a set of results, which explore the stability and the activation barriers for transitions between various magnetic arrangements under bias, as well as the effect of the model parameters on the physical properties of the system. Finally, we carry out a numerical test to see whether or not the torques in these opene-boundary nonequilibrium systems are conservative.

II. THE METHOD

A. General idea

Our scheme for studying current-induced dynamical effects of the magnetization in atomic-sized nanostructures is a generalization of the combined quantum-classical dynamical methods used in electromigration problems.[8] Here we treat the magnetic degrees of freedom as classical variables and the conduction electrons as a quantum system. This is appropriate when the magnetic moment (MM) arises from some deep orbital levels, such as in the case of rare earth ferromagnets, but it may appear questionable for magnetic transition metals (Fe, Co, and Ni), where the *d* electrons responsible for the moment also take part in the conduction.[9] However, since the Coulomb energy is orders of magnitude larger than any energies connected with the electron flow, it is safe to assume that only the direction of the local atomic MM is affected by the current, not its magnitude. This effectively is an adiabatic approximation, in the spirit of the Born-

Oppenheimer approximation for the nuclear dynamics, where now the orientation of the local MMs is a slow variable compared with the internal electron-electron interactions that set the magnitude of the MMs.[10,11] The Hamiltonian for the combined conduction-electron/MM system can be then written in general as

$$H(\{\phi\}) = H_e + V_m(\{\phi\}), \tag{1}$$

where we have isolated the "free" electron Hamiltonian H_e from the term $V_m(\{\phi\})$, describing all the magnetic interactions. In this framework the local moments are uniquely specified by a set of angles $\{\phi\}$ with respect to a given direction.

We may now write down the generalized forces (in this case, torques) conjugate to the classical variables $\{\phi\}$:

$$T = -\langle\Psi|\frac{\partial H(\{\phi\})}{\partial \phi}|\Psi\rangle, \tag{2}$$

where $|\Psi\rangle$ is a state vector of the electronic system. Equation (2) has the appearance of the usual Hellmann-Feynman theorem for stationary states. However, it is valid in general dynamical situations, for systems driven arbitrarily far from equilibrium.[12,13]

Equations (1) and (2), combined with an appropriate method for calculating the nonequilibrium electron state vector $|\Psi\rangle$, and therefore the current, are the basis for our method for describing the interplay between transport and magnetic properties. In this work, we seek to map out the activation energy barriers for magnetic rearrangements, in order to determine the preferential magnetic configurations of the system and to study transitions between them. We achieve that as follows. First, we seek the stable configurations. We evaluate the nonequilibrium state vector $|\Psi\rangle$, in a one-electron picture, for a given initial MM configuration $\{\phi^0\}$ by solving the scattering problem associated with the Hamiltonian $H(\{\phi^0\})$. Then, by using Eq. (2) the torques for that configuration are calculated. Static iterative relaxation of the torques, which involves recalculating the self-consistent current-carrying electronic structure and the torques, is carried out as follows:

$$\{\phi^n\} = \{\phi^{n-1}\} + \alpha T^{n-1}, \tag{3}$$

where $\{\phi^n\}$ and T^{n-1} are, respectively, the MM configuration and the torques on the nth iteration. A positive value of α guarantees that the $T=0$ solution corresponds to a stable magnetic configuration $\{\Phi\}$.

Once the stable magnetic configurations are found, we can calculate the activation energy barriers for thermally activated transitions between two different configurations $\{\Phi^{initial}\}$ and $\{\Phi^{final}\}$. We then choose one of the classical dynamical variables ϕ_j as the reaction coordinate and rotate it from its initial value $\phi_j^{initial}$ to its final value ϕ_j^{final}. At every step on the way the torques acting on all other MMs are kept relaxed to zero. The work done by the classical degrees of freedom during this quasistatic transition is then obtained by integrating the torque on the reaction coordinate ϕ_j over the migration path. The work done over the full transition is

$$W = -\int_{\Phi^{initial}}^{\Phi^{final}} T_j d\phi_j. \tag{4}$$

The energy barrier profile, on the other hand, is given by

$$W(\Phi_j) = -\int_{\Phi^{initial}}^{\Phi_j} T_j d\phi_j, \tag{5}$$

where $\Phi_j=\{\phi_1(\phi_j),\phi_2(\phi_j),\ldots,\phi_j,\ldots,\phi_N(\phi_j)\}$ is the magnetic configuration, for a given ϕ_j, defined by the condition $T_i=0$ for every $i\neq j$.

B. Transport method

The Keldysh nonequilibrium Green's function (NEGF) method is used here for describing the transport.[14,15] We expand the Hamiltonian $H(\{\phi\})$ and the one-electron wave functions in a localized atomic orbital basis set, and we decompose our system into two current (or voltage) probes sandwiching a central region. For an open current-carrying system H can be written as

$$H = H_L + H_R + H_C + H_{LC} + H_{RC}, \tag{6}$$

where we have introduced the Hamiltonian for the left- (right-) hand side probe $H_L=H_L(\{\phi\})$ $[H_R=H_R(\{\phi\})]$, that for a central scattering region $H_C=H_C(\{\phi\})$, and the coupling matrix between the left (right) contact and the scattering region $H_{LC}=H_{LC}(\{\phi\})$ $[H_{RC}=H_{RC}(\{\phi\})]$. The latter are indeed spin-polarized operators, i.e., $H=\Sigma_\sigma H^\sigma$, but for the sake of simplicity of the expression we skip the spin index σ in the following formulas, thus referring to either of the spin components.

The NEGF method allows us to map this, in principle infinite problem (H_R and H_L are infinite matrices), on an auxiliary finite problem. The key observation is that one can describe the effects of the current/voltage probes over the scattering region by means of their corresponding self-energies Σ_L and Σ_R. These are non-Hermitian matrices, which contain all information about the electronic structure of the probes and their occupation. They can be written as

$$\Sigma_L = H_{LC}^\dagger g_L H_{LC}, \quad \Sigma_R = H_{RC} g_R H_{RC}^\dagger, \tag{7}$$

where we have defined the surface Green's function (GF) for the left- (right-) hand-side probe $g_R(g_L)$. Hence the "effective Hamiltonian" of the scattering region in the presence of the current/voltage electrodes is written as

$$H_{eff} = H_C + \Sigma_L + \Sigma_R. \tag{8}$$

Note that this is a finite non-Hermitian matrix. Consequently, the number of electrons in the scattering region is not conserved.

Now we can construct the retarded GF associated with the scattering region plus the leads

$$G(E) = \lim_{\zeta\to 0^+}[(E+i\zeta) - H_C - \Sigma_L - \Sigma_R]^{-1}, \tag{9}$$

and the associated (nonequilibrium) density matrix

$$\rho = \frac{1}{\pi}\int_{-\infty}^{\infty} dE[n_L(E)\,\eta_F^L(E) + n_R(E)\,\eta_F^R(E)], \qquad (10)$$

where $n_A(E)=G(E)\Gamma_A(E)G^\dagger(E)$ are the partial density of state operators for electrons originating from each lead $(A=R,L)$, $\Gamma(E)=i[\Sigma(E)-\Sigma^\dagger(E)]/2$ is the non-Hermitian part of the self-energy, and $\eta_F^A(E)=\eta_F(E-\mu_A,T)$ are the corresponding Fermi distribution function for the electron reservoirs with chemical potential μ_A at some finite temperature T.

Under our basic assumption of "reflectionless" leads we can decouple the subsystems of electrons originating from the left and the right lead and treat them as separate statistical systems with electrochemical potentials $\mu_{L(R)}$. In equilibrium $\mu_L=\mu_R=\mu$, and a finite bias V is introduced as $\mu_{L(R)}=\mu\pm|e|V/2$, so that the electron flow is from the left to the right lead for $V>0$. Thus the bias V is assumed not to change the electronic structure of the leads, but only to rescale the energy levels. In practice V is introduced as a rigid shift of lead-Hamiltonian on-site energies

$$H_{\mathrm{L/R}} \to H_{\mathrm{L/R}} \pm \frac{V}{2}\mathcal{I}, \qquad (11)$$

where $\mathcal{I}$ is the identity matrix for the respective lead.

Self-consistency in our calculation is introduced by assuming that for a given magnetic configuration $\{\phi\}$ the Hamiltonian H_C depends solely on the scattering region density matrix $H_C=H_C[\rho]$. This is equivalent to assuming that the underlying electronic structure theory is a density-based theory, such as Hartree-Fock or density functional theory. In this case the set of equations (8), (9), and (10) defines the self-consistent procedure. First one computes the scattering region GF [Eq. (9)] for $H_C[\rho_0]$ evaluated at an initial density matrix ρ_0. Then from the GF a new charge density ρ_1 is calculated and used to construct the new Hamiltonian $H_C[\rho_1]$. This procedure is iterated until reaching self-consistency, that is, until $\rho_{n+1}=\rho_n$.

Finally, from the converged GF the net current is calculated as[14,15]

$$I(V) = \frac{e}{h}\sum_\sigma \int_{-\infty}^{\infty} dE[\,\eta_F^L(E) - \eta_F^R(E)] \times \mathrm{Tr}[\Gamma_L(E)G^\dagger(E)\Gamma_R(E)G(E)]^{(\sigma)}, \qquad (12)$$

where we have summed over the spin index σ.

C. The model

The techniques described in the previous sections are general and can be applied to a large class of Hamiltonians. In this work we focus our attention on a simplified model, which contains the fundamental ingredients for describing a current-carrying magnetic point contact, but at the same time does not present massive computational overheads. The structure we investigate is schematically represented in Fig. 1. It consists of two semi-infinite leads with a simple cubic lattice structure and a 3×3-atom cross section connected through a linear chain of three atoms. Each atom carries a local magnetic moment, our classical quantities, arising from the deeply localized d electrons. The magnetic configuration of the leads is fully polarized (all MMs in a given lead point in the same direction) and we investigate the situation where the magnetizations of the two leads are opposite to each other. In contrast, the three MMs of the atoms in the chain are allowed to rotate. A given magnetic configuration of the chain is thus described by the three angular coordinates (ϕ_1,ϕ_2,ϕ_3) with respect to the x axis, which is set parallel to the magnetization of the left lead, i.e., $\phi=0$ $(\phi=\pi)$ for a MM aligned parallel to the magnetization of the left (right) lead. We consider rotations of MMs only in the x-y plane thus neglecting the longitudinal angle (as in a Bloch wall). The alternative choice would be to consider MM rotations in the x-z plane (a Néel wall), but as far as we neglect the magnetocrystalline anisotropy, these two models are identical.

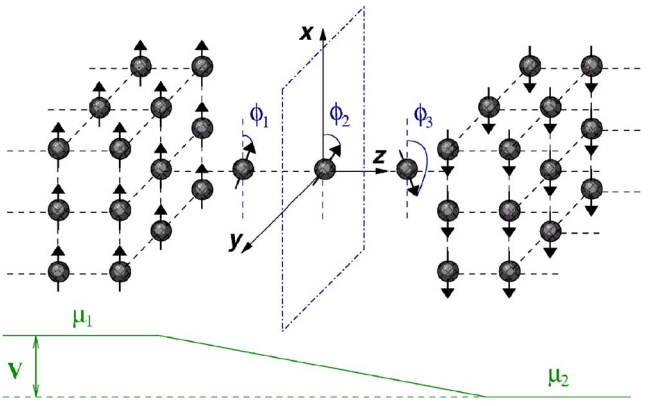

FIG. 1. (Color online) Scheme of the point contact.

The current is carried by electrons belonging to an s band, which is described by means of a single-orbital (plus spin) TB model. We neglect spin noncollinearity of the current-carrying electrons, since the time needed to cross the constriction is considerably shorter than their spin-relaxation time. The Hamiltonian of Eq. (1) is therefore explicitly written as

$$H(\{\phi\}) = \sum_{i,j}[(H_e)_{ij} + (V_{\mathrm{int}})_{ij}]c_i^\dagger c_j + V_{\mathrm{classical}}(\{\phi\}), \qquad (13)$$

where $c_i^\dagger$ and c_j are creation and annihilation operators for electrons at the atomic sites i and j, respectively. The matrix elements of the free electron part are those of a nearest-neighbor TB model

$$(H_e)_{ij} = [\epsilon_0 + U(\rho_i - \rho_i^0)]\delta_{ij} + \gamma\delta_{i,j\pm1}, \qquad (14)$$

where ϵ_0 is the on-site energy, γ is the hopping parameter, U is the on-site Coulomb repulsion, ρ^0 the reference on-site charge corresponding to the neutral free atom, and ρ is the self-consistent local charge. The potential V_m of Eq. (1) has now been separated in two parts: V_{int} and $V_{\mathrm{classical}}$. The interaction between conduction electrons and the local MMs is contained in V_{int}, which in our model reads

$$(V_{\text{int}})_{ij} = -s_i \frac{J}{2} \cos(\phi_i)\delta_{ij}, \tag{15}$$

where $s_i = \rho_i^{\uparrow} - \rho_i^{\downarrow}$ is the local spin polarization of the s electrons at site i and J is the exchange parameter. Therefore V_{int} describes a Heisenberg-type interaction between the local classical MMs and the current carrying s electrons. Finally, the classical term $V_{\text{classical}}$ parametrizes the interaction between local MMs. Here we assume a Heisenberg spin-spin interaction

$$V_{\text{classical}} = -\frac{J_{dd}}{2}\sum_{i,j} \boldsymbol{S}_i \cdot \boldsymbol{S}_j = -\frac{J_{dd}}{2}\sum_{i,j} \cos(\phi_i - \phi_j), \tag{16}$$

where J_{dd} is the intersite exchange integral and we have assumed normalized classical spin $|\boldsymbol{S}_i| = 1$, in such a way that $|\boldsymbol{S}_i|$ is incorporated in the definitions of J and J_{dd}. In summary, our model is that of s conduction electrons exchange-coupled to local MMs, in turn described by a Heisenberg-type energy. This is usually known as the s-d model.[16]

The torque experienced by the ith local MM in the chain is then obtained from Eq. (2) and reads

$$T_i = -\frac{J}{2} s_i \sin(\phi_i) - \frac{J_{dd}}{2}[\sin(\phi_i - \phi_{i-1}) + \sin(\phi_{i+1} - \phi_i)], \tag{17}$$

where $i = 1,2,3$, and we have defined $\phi_0 \equiv 0$, $\phi_4 \equiv \pi$ since the magnetization of the two leads is considered pinned in an antiparallel arrangement.

In this simple model the surface GF (at a general complex energy E) of the leads have an analytical form. In reciprocal space for complex energy in the upper half plane [$\text{Im}(E) > 0$]

$$g(E,\boldsymbol{k}) = \frac{E - \epsilon(\boldsymbol{k}) - \sqrt{[E - \epsilon(\boldsymbol{k})]^2 - 4\gamma^2}}{2\gamma^2}, \tag{18}$$

where $\epsilon(\boldsymbol{k})$ is the energy, as a function of transverse wave vector (in appropriate units) $\boldsymbol{k} = (k_x, k_y)$ with $k_x = 1, \ldots, N_x$, $k_y = 1, \ldots, N_y$ for an $(N_x \times N_y)$-atom square monoatomic slab in a nearest-neighbor orthogonal TB s-band model,

$$\epsilon(\boldsymbol{k}) = \epsilon_0 - 2|\gamma|\cos\left(\frac{k_x \pi}{N_x + 1}\right) - 2|\gamma|\cos\left(\frac{k_y \pi}{N_y + 1}\right). \tag{19}$$

The expression of Eq. (18) is then expanded over the real-space basis[17] and used in the matrix equation for the self-energies. The definition of the complex square-root is given in Ref. 18.

III. RESULTS

Here we investigate the magneto-dynamics of atomic point contacts, and in particular of the model structure described in Fig. 1. The TB parameters are $\epsilon_0 = -3$ eV, $\gamma = -1$ eV, $U = 12$ eV, which gives a large bandwidth for the s electrons and provides local charge neutrality as expected in a metal. For the exchange parameters we investigate the range $0 \leqslant J \leqslant 3$ eV and $0 \leqslant J_{dd} \leqslant 5$ eV. However, we have identified the values $J = 1$ eV and $J_{dd} = 50$ meV as a realistic choice for simulating the main physics of magnetic transition metals,[16,19,20] and we will refer to those values as the "realistic parameters."

We start our analysis with studying DW migration in the three-atom chain. As in Fig. 1, the magnetic moments of the leads are in the antiparallel configuration, so that a DW nucleates in the chain. We then investigate the displacement of the Bloch wall from the interface between the first and the second atom in the chain to that between the second and the third (generated by a rotation of the magnetic moment of the middle atom). These simulations use the realistic parameters given above, so they can be related to point contact experiments.[21] Both the cases of spatially symmetric and asymmetric chains are studied. Then we explore the effect of varying the strength of the exchange parameters and identify three different regimes. Finally, we revisit the problem of whether or not generalized forces away from equilibrium are conservative, then demonstrate numerically that the torques in the present system under current flow are not conservative.

A. Domain wall migration

By performing numerical minimization of all the torques, exerted on the MM in the constriction, with various initial conditions, we determined that all eight collinear arrangements, such as (0,0,0), $(0,0,\pi)$, $(0,\pi,\pi)$, $(\pi,\pi,0)$, etc., are stable zero-torque magnetic configurations and we have studied various transitions between them (see Fig. 10). In particular, we have investigated in detail the quasistatic migration of an abrupt DW within the atomic chain, i.e., the transition between the $(0,0,\pi)$ and $(0,\pi,\pi)$ magnetic configurations, achieved by rotation of $\boldsymbol{M}_2$ (which is the MM associated with the spin S_2) as described above. Physical characteristics of this process as function of ϕ_2 are presented in Fig. 2. It is observed that during the rotation of $\boldsymbol{M}_2$ its neighboring MMs experience small tilts from the collinear alignment and after a turning point fall back to their initial state [Fig. 2(a)]. The intersite exchange coupling is not strong enough to induce spin flips of the neighboring MM along with the one that is rotated and even hypothetical values of J_{dd} up to 0.4 eV do not change this picture (see Fig. 6). This observation suggests that the dynamical processes of the MMs in the constriction can be decomposed into series of single MM rotations. Due to the specific spatial symmetry of the atomic geometry we have the relation

$$\phi_3(\phi_2) = \pi - \phi_1(\pi - \phi_2) \tag{20}$$

and unless this symmetry is deliberately broken in our discussion we will always refer only to $\phi_1(\phi_2)$.

The torque T_2, computed as a function of ϕ_2 [Fig. 2(c)] at every point on the way, is interpolated and integrated according to Eq. (4) to determine the effective energy barrier for the DW migration

$$W(\phi_2) = -\int_0^{\phi_2} T_2 d\phi_2'. \tag{21}$$

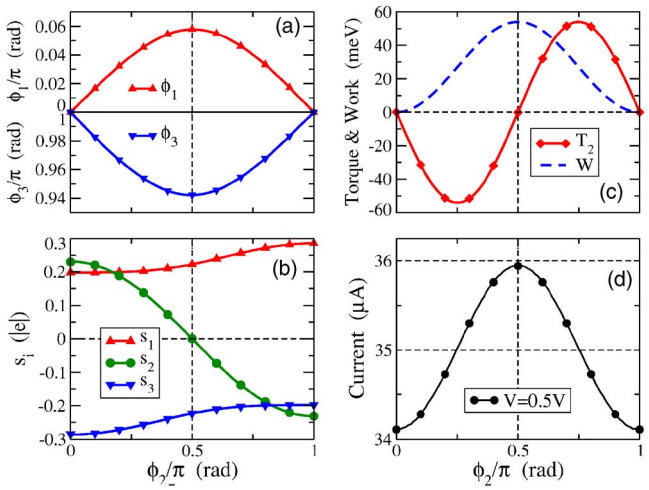

FIG. 2. (Color online) Typical calculation of microscopic properties during DW migration in the contact (for $J=1$ eV, $J_{dd}=50$ meV) as a function of the "reaction coordinate" ϕ_2: (a) the stable angular variables ϕ_1 and ϕ_3; (b) the three on-site spin polarizations $s_i=\rho_i^{\uparrow}-\rho_i^{\downarrow}$; (c) torque and work, performed by the MM; (d) net current at $V=0.5$ V. The voltage in panels (a)–(c) is zero.

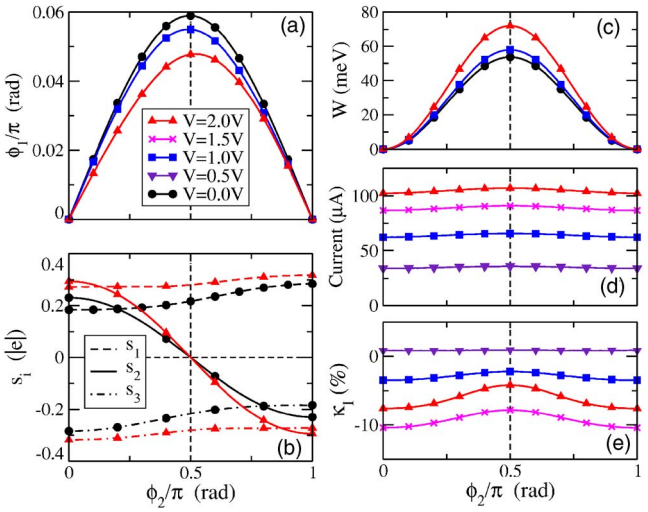

FIG. 3. (Color online) Effect of the external bias on the microscopic properties of the contact as function of ϕ_2: (a) the zero-torque positions of ϕ_1 [ϕ_3 obeys Eq. (20)]; (b) the on-site spin polarizations $\{s_i=\rho_i^{\uparrow}-\rho_i^{\downarrow}\}_{i=1,2,3}$; (c) the work profile; (d) the total net current, and (e) its polarization $\kappa_I=(I_{\uparrow}-I_{\downarrow})/(I_{\uparrow}+I_{\downarrow})$.

Because of the specific geometric and time-reversal symmetries of the system, the two states $(0,0,\pi)$ and $(0,\pi,\pi)$ are macroscopically identical at any bias. Thus the calculated energy barrier between them is symmetric and the total work $W(\pi)$ for the quasistatic process is zero [Fig. 2(c)]. The activation energy for this process in our TB parametrization is 54 meV. It is found that the conductance of our system depends on the alignment of the MM and in this case the net current shows a symmetric bell-shaped dependence on ϕ_2 [Fig. 2(d)]. For this case ($V=0.5$ V), the conductance varies from $1.76e^2/h$ at the collinear states $\phi_2=0,\pi$ to a maximum of $1.86e^2/h$, reached at $\phi_2=\pi/2$.

Further, it is observed that the external bias, driving a spin-polarized current, suppresses the response of $\phi_{1,3}$ to the motion of ϕ_2 [Fig. 3(a)] but enhances the onsite polarizations [Fig. 3(b)] as well as the energy barrier [Fig. 3(c)]. At any finite temperature, this phenomenon would manifest itself as suppression, with increasing bias, of the frequency of DW transitions back and forth between the two stable magnetic configurations. The net current profile is slightly sharpened as the bias increases [Fig. 3(d)] and it also becomes more spin-polarized due to the increased misalignment of the correspondent spin-polarized bands in the two leads [Fig. 3(e)].

B. Nonuniform contact

Current-induced relaxation of the atomic positions can break the spatial symmetry in point contacts similar to ours[8] and substantially weaken the stability of these systems. To investigate the effect of a small asymmetry in the contact geometry on the migration barrier for the DW, we map the displacement of the middle atom from its symmetric position onto a small variation of hopping integrals between the middle atom and its neighbors in the chain

$$\gamma_{12}=\gamma(1+\delta), \quad \gamma_{23}=\gamma(1-\delta). \tag{22}$$

This results in breaking the symmetry about $\phi_2=\pi/2$ of the effective energy barrier observed in all our previous calculations (Fig. 4). The total work for the $(0,0,\pi)\rightarrow(0,\pi,\pi)$ transition is negative, thus the internal energy of the classical MM is increased. The degeneracy of the $(0,0,\pi)$ and $(0,\pi,\pi)$ state is lifted, as the spatial symmetry, associated with a reflection plane at $z=0$, is no longer present. When the hopping parameters are altered by $\delta=5\%$, as if the middle atom is slightly shifted to the left, the $(0,\pi,\pi)$ configuration becomes energetically preferable, alternatively, $\delta=-5\%$ favors the $(0,0,\pi)$ state, with all the physical properties being invariant to the transformation $\{\delta,\phi_2\}\rightarrow\{-\delta,(\pi-\phi_2)\}$ (Fig. 4).

We present the typical microscopic properties in Fig. 5. The effective ferromagnetic coupling between the MMs is

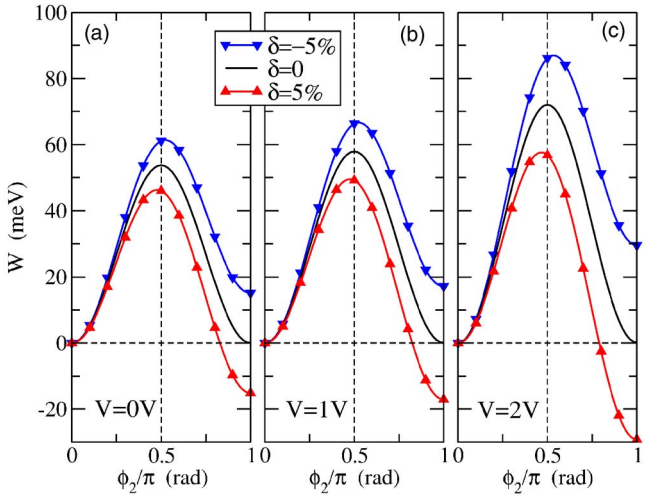

FIG. 4. (Color online) Effect of an asymmetry in the hopping integrals in the three-atom chain with $\delta=\pm0.05$ on the barriers for $(0,0,\pi)\rightarrow(0,\pi,\pi)$ transition at different bias: (a) $V=0$ V; (b) $V=1$ V; (c) $V=2$ V.

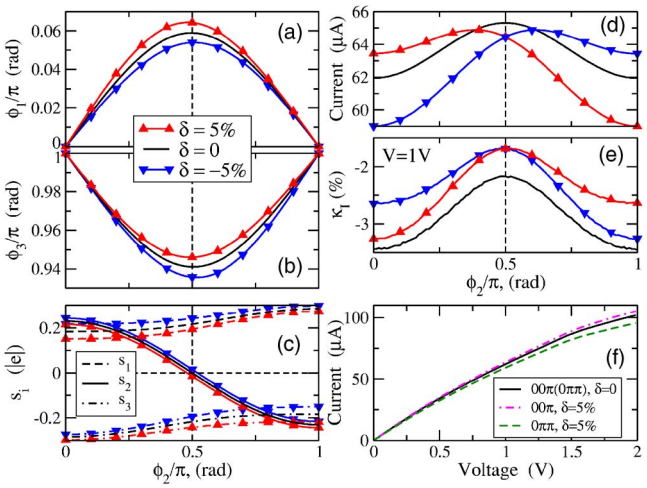

FIG. 5. (Color online) Effect of an asymmetry in the hopping integrals with $\delta=\pm 5\%$ on the microscopic properties of the contact: (a) and (b) angles $\phi_{1,3}$ [note that the symmetry relation in this case becomes $\phi_3(\phi_2,\delta)=\pi-\phi_1(\pi-\phi_2,-\delta)$]; (c) the on-site spin-polarization; (d) and (e) net current and its spin-polarization at $V=1$ V. The bias on (a), (b), and (c) is $V=0$ V. On panel (f) are the I-V characteristics for the $\{0,0,\pi\}$ and $\{0,\pi,\pi\}$ states. It is also observed that $I(V,\delta,\{00\pi\})=I(V,-\delta,\{0\pi\pi\})$.

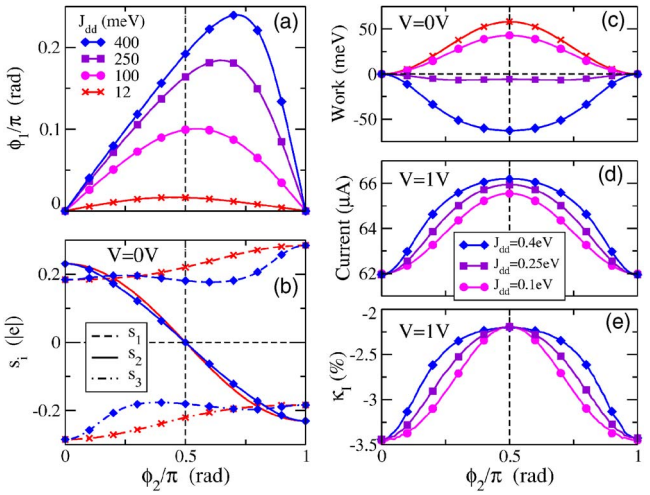

FIG. 6. (Color online) Effect of the strength of the intersite coupling J_{dd} on the microscopic properties (as in Fig. 3) in equilibrium (a)–(c) and net current properties at $V=1$ V [(d) and (e)].

strengthened by the enhanced electronic hopping and the on-site polarizations of all the atoms shift almost rigidly as the middle atom is brought toward one or the other of the leads. The net current shows significant asymmetry from the regular bell-shaped dependence on ϕ_2 and the more stable configuration is always found to be less conducting [Fig. 5(d)]. The I-V characteristics of the previously degenerate $(0,0,\pi)$ and $(0,\pi,\pi)$ states is split into two branches, whose displacement increases with voltage [Fig. 5(f)] and reaches 10% for $V=2$ V. Thus we expect DW migrations within the constriction, in the case of small deviations from a uniform geometry, to be accompanied by random-telegraph-noise-like variations in the net current. The interplay between the current-induced relaxation of the magnetic and mechanical degrees of freedom is the subject of work in progress.

C. Mapping out the parameter space

The torques defined in Eq. (17) depend explicitly on the exchange parameters J, J_{dd} and the balance of these two coupling mechanisms determines the spin dynamics in the constriction. Figures 6(a)–6(c) describe the variation of the equilibrium magnetic properties of the $(0,0,\pi)\rightarrow(0,\pi,\pi)$ transition as the intersite exchange strength J_{dd} is varied. The effect of the greater J_{dd} is increased disalignments of the two neighboring MM $\phi_{1,3}$ following the rotation of ϕ_2 [Fig. 6(a)]. Because of this the corresponding spin-polarizations $s_{1,3}$ (but not s_2) are slightly affected [Fig. 6(b)] as a result of the stronger coupling. The typical bell shape of the current vs ϕ_2 is broadened as J_{dd} increases [Fig. 6(d)] due to the fact that stronger intersite exchange coupling tends to make the three MMs in the contact more uniformly distributed in angle, which makes the contact better-conducting for any ϕ_2. The current is somewhat less polarized in the case of stronger intersite coupling [Fig. 6(e)].

The graph in Fig. 7 describes the distribution of stability patterns of the three MMs in the constriction as a function of the exchange parameters, based on a study of the DW migration barrier. We can distinguish three different regimes depending on the values of the exchange parameters: (1) *magnetostatic regime* associated with the presence of two stable magnetic states, for which $\phi_2=\pm\pi/2$; (2) *mixed regime*: four stable configurations, two in each half-plane for which $0<\phi_2<\pi/2$ and $\pi/2<\phi_2<\pi$; and (3) *current-driven regime*: eight stable configurations, namely all the collinear MM alignments (0,0,0), (π,π,π), $(0,0,\pi)$, $(0,\pi,\pi)$, $(\pi,0,0)$, $(\pi,\pi,0)$, $(0,\pi,0)$, $(\pi,0,\pi)$ (see Fig. 10). The

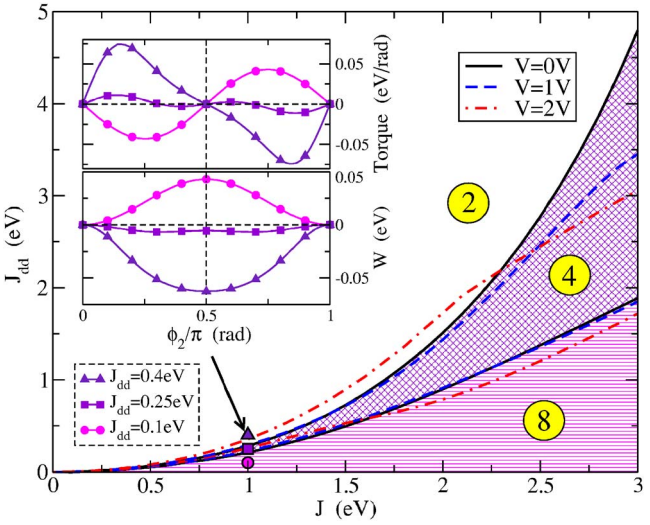

FIG. 7. (Color online) Diagram showing the three regions, with two, four, and eight stable magnetic configurations respectively (see text), in a J–J_{dd} cut of the parameter space. The boundaries between the three regimes are calculated from the properties of the $(0,0,\pi)\rightarrow(0,\pi,\pi)$ transition (see inset). The dashed lines correspond to voltages of 1 and 2 V.

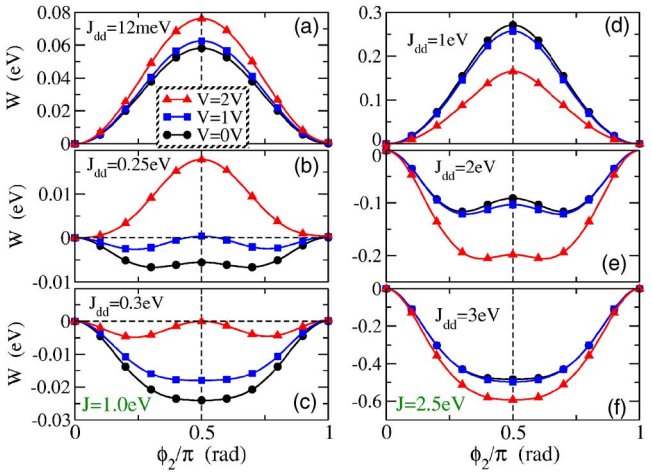

FIG. 8. (Color online) The biased energy barriers for the transition $(0,0,\pi)\rightarrow(0,\pi,\pi)$ at different voltages V=0,1,2 V, J=1.0 eV (left) and J=2.5 eV (right), and for three values of J_{dd} (one in each of the ranges, discussed in the text): (a) J_{dd}=12 meV; (b) J_{dd}=0.25 eV; (c) J_{dd}=0.3 eV; (d) J_{dd}=1 eV; (e) J_{dd}=2 eV; (f) J_{dd}=3 eV.

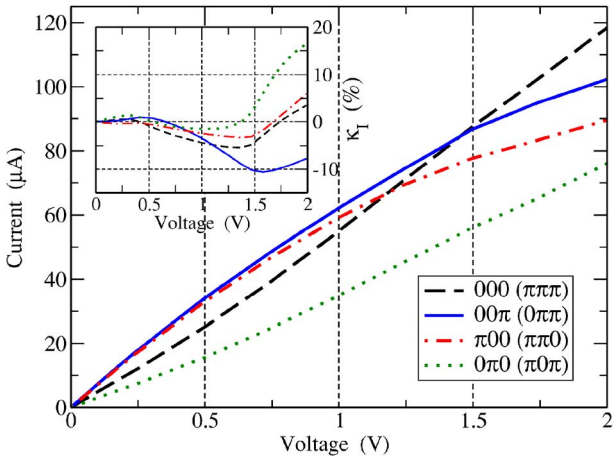

FIG. 9. (Color online) The current-voltage characteristics at all stable collinear alignments for the MM in the chain. The inset represents the correspondent spin-polarization of the net current $\kappa_I=(I_\uparrow-I_\downarrow)/(I_\uparrow+I_\downarrow)$. It is a nonmonotonic function of the bias.

last case is confirmed by full torque relaxations at various initial conditions. It should be noted that stability of the two unipolarized collinear configurations is also found above the boundary in Fig. 7, but they are then only accessible once the system is trapped within very narrow regions of $\{\phi\}$ space. Our main observation is that the collinear configurations are the only form of stability of the magnetic chain in the contact for a range of exchange parameters around the realistic values, defined earlier. Thus, even though our calculations in the previous and in the next section use J_{dd}=50 meV and J =1 eV, the qualitative features of the results may be expected to hold for a range of values of J_{dd} in the region of tens of meV and $J\gtrsim 0.5$ eV.

It is observed that the bias, driving a spin-polarized current, is able to distort the boundaries between these three regions significantly (Fig. 7, dashed lines refer to V=1, 2 V). The effect of the bias on the migration energy-barrier profile has been studied for different values of the exchange parameters and reported for two representative cases, J=1 eV and J=2.5 eV (Fig. 8). The overall observation is that for $J\lesssim 1.5$ eV (the realistic regime) increasing bias (current) enforces the barrier, while for $J\gtrsim 2.5$ eV the bias suppresses the barrier. For intermediate values of J the barrier shows a nonmonotonic behavior with bias.

D. Current-voltage characteristics

The current-voltage characteristics of the system at all the different stable alignments of the MM in the chain are presented in Fig. 9. All the I-V curves are symmetric about the origin and form four separate branches as the eight possible stable magnetic states are 4×2 degenerate. This is due to the specific spatial and time-reversal symmetry of the atomic point contact. The slopes of the I-V curves cannot be directly related to the number of DWs in the constriction (three for the $\{0,\pi,0\}$ and $\{\pi,0,0\}$; one for $\{0,0,0\}$ and $\{0,0,\pi\}$ states). Nevertheless, the least steep curve does correspond to the highest number of domain walls present within the chain. As soon as the DW in the chain migrates toward the leads (as in the $\{0,\pi,0\}$ to $\{\pi,0,0\}$ transition) the conductance increases. We conclude that microscopic magnetization reversals in the constriction could be causing massive current variations (of up to 50%) at a given bias. At a given finite temperature this would result in a random telegraph noise in conductance measurements and such effects have been observed experimentally.[7,21,22]

Figure 10 represents the work for a series of 1 MM rotations. The sequence of transitions goes through every stable magnetic configuration once and returns to the initial state. In equilibrium the depths of the wells in this graph correspond to the relative energies of our system in various stable magnetic states with respect to the initial one. Thus $(0,\pi,0)$ and $(\pi,0,\pi)$, which have three abrupt DWs and are the least conducting states, are found to be the most stable among the collinear alignments. It is observed that the external bias has

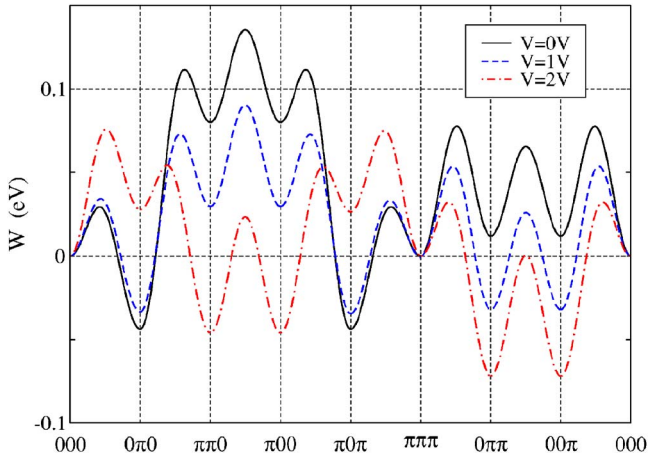

FIG. 10. (Color online) Work for successive transitions between the eight stable magnetic configurations at different bias V=0,1,2 V.

a non-trivial effect on the effective energy barriers for these transitions. The total work for the closed loop cancels out for any bias. This, however, is not an indication of conservativeness of the current-induced torques [Eq. (2)] but is rather an artifact of the specific symmetries in this certain closed path, which includes all the states and can be decomposed into two subloops going through identical states in opposite directions.

There are $12=(5\times2+2)$ one-MM-rotation transitions between non-identical pairs of stable collinear alignments, out of which we distinguish $5+2=7$ different transitions. The average activation barrier at equilibrium is 71 meV with a variance of 36 meV and it depends non-monotonically on the bias: 65.6 meV at 1 V and 68 meV at 2 V. These values for the activation barriers suggest switching frequencies, and hence random telegraph noise in the current, in the microwave range at room temperature.

E. Are the torques conservative?

The question if, and under what conditions, forces under steady-state current are conservative remains an open fundamental problem in the theory of transport.[23] A thermodynamic formulation of forces under nonequilibrium steady-state conditions, proposed in Ref. 18, leads to the explicit identification of a thermodynamic potential for electromigration.[24] However, as a consequence of the infinite nature of open-boundary systems, this potential involves a conditionally convergent real-space summation. If the sequence of terms in this summation remains invariant along a given path in the configuration space of the system, then along that path, current-induced generalized forces are rigorously expressible as gradients of a scalar potential and are therefore conservative. The possibility remains open, however, that the order of terms in the conditionally convergent sum may change, as specific points, or manifolds, in configuration space are traversed.[24] This constitutes an effective breakdown of the Born-Oppenheimer approximation, with the consequence that paths that span such points are nonconservative.[24]

We now carry out a numerical test to see whether or not the torques in Eq. (17) are conservative in the present current-carrying system. The work for a set of transitions between collinear MM configurations, performed by rotation of a single MM, which form a closed loop, is calculated for different voltages. The full work for three different loops of four consecutive transitions as a function of the applied voltage is presented in Fig. 11. A significant variation of the closed-loop work with bias is observed.

In order to resolve the numerical error we have performed a series of tests with different levels of accuracy. We recognize several sources of numerical error: (1) the level of convergence of the density matrix $\delta\rho$; (2) the fineness of the energy mesh for the charge density [Eq. (10)] integration δE; (3) the level of torque relaxation δT; (4) the angular mesh for the torque integration which results into the work. As the torque in the current-driven regime is a very smooth function of the reaction coordinate [Fig. 2(c)], we have found the angular mesh fineness insignificant for the value of the integral Eq. (5). The effect of the rest of the accuracy parameters

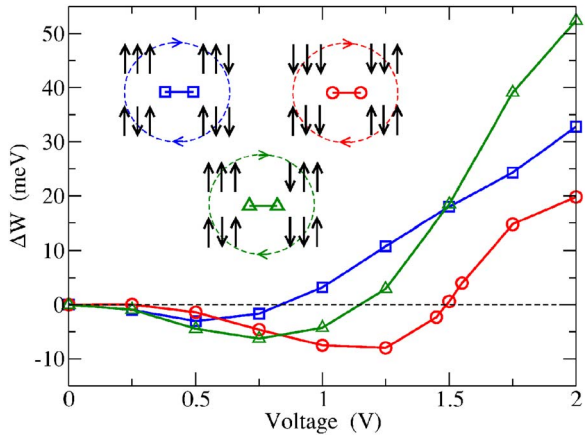

FIG. 11. (Color online) Dependence of closed-loop work on the voltage.

on the closed loop work (see the loop $\{\pi\pi\pi\text{-}\pi\pi0\text{-}0\pi0\text{-}0\pi\pi\text{-}\pi\pi\pi\}$ in Fig. 11) is summarized in Table I.

The results in Table I suggest that the main observation of nonzero work for a closed-loop set of transitions is not substantially affected by variations of 1–2 orders of magnitude about the chosen level of accuracy. Thus we see that in the present case, along the selected closed paths, we have an explicit example of nonconservative generalized nonequilibrium forces.

IV. CONCLUSIONS

In conclusion, we have proposed a microscopic quantum-classical approach for computing the current-induced torques on the local magnetization in ferromagnetic point contacts under bias. Our method employs an *s-d* model for the electronic structure and NEGF technique for describing the electronic transport. The directions of the local MMs are mapped onto classical degrees of freedom. We apply this method to a specific atomic structure, which consists of a monoatomic chain, bridging over two semi-infinite leads with opposite magnetizations, so that at least one magnetic DW is formed within the constriction. We then investigate the stability of various magnetic configurations, involving multiple DWs, and the effect of bias driving a spin-polarized current, on the energy-barrier for the DW migration. For realistic values of exchange parameters only the collinear MM arrangements are stable. These configurations carry different (by up to 50%) net currents, and the average activation barrier for transitions is about 65–70 meV with variance of 20–40 meV,

TABLE I. The work (in meV) for the loop $\{\pi\pi\pi\text{-}\pi\pi0\text{-}0\pi0\text{-}0\pi\pi\text{-}\pi\pi\pi\}$ as a function of the accuracy parameters (in relative units). The value of the bias V is given as a subscript.

$(\delta\rho,\delta E,\delta T)$ (%)	$W_{0\ \mathrm{V}}$	$W_{0.5\ \mathrm{V}}$	$W_{1\ \mathrm{V}}$	$W_{1.5\ \mathrm{V}}$	$W_{2\ \mathrm{V}}$
(100,100,100)	0.0001	−1.407	−7.454	0.601	19.81
(100,20,100)	0.0001	−1.290	−7.361	−0.036	19.79
(1,100,2)	0.0406	−1.300	−7.356	0.662	19.88

depending on the bias. Therefore random telegraph noise in current with significant amplitude could be related to thermally activated MM rearrangements within the constriction. We have also found that geometrical asymmetries in the atomic structures (which could be induced by the current)[8] affect the symmetry of the activation barrier for DW migration, pinning the DW to a preferential spatial position, which corresponds to lower conductivity of the structure.

The observation that the collinear MM alignments are the only stable magnetic states and the fact that direct intersite interaction is not able to induce flips in the neighboring MMs, as one MM in the chain is quasistatically rotated, enabled us to calculate the work for series of rearrangements of the MMs in the constriction, involving single-MM rotations. Thus, we address numerically the long-standing question of the conservativeness of the current-induced forces (torques, in our case) in open-boundary nonequilibrium system. We have found numerical evidence that the work for various closed-loop paths is not zero, but varies nonmonotonically as the system is driven away from equilibrium. Hence generalized current-induced forces in our present system are not conservative, at least in the section of the configuration space spanned by the present calculations.

ACKNOWLEDGMENTS

This work is sponsored by the Irish Higher Educational Authority under the North South Programme for Collaborative Research. M.S. is grateful to A. R. Rocha for the transport code kernel and helpful discussions.

*Email address: sanvitos@tcd.ie

[1] P. Bruno, Phys. Rev. Lett. **83**, 2425 (1999).
[2] M. N. Baibich, J. M. Broto, A. Fert, F. Nguyen Van Dau, F. Petroff, P. Etienne, G. Creuzet, A. Friederich, and J. Chazelas, Phys. Rev. Lett. **61**, 2472 (1988).
[3] G. Binasch, P. Grünberg, F. Saurenbach, and W. Zinn, Phys. Rev. B **39**, 4828 (1989).
[4] J. Slonczewski, J. Magn. Magn. Mater. **159**, L1 (1996).
[5] W. H. Rippard, M. R. Pufall, S. Kaka, S. E. Russek, and T. J. Silva, Phys. Rev. Lett. **92**, 027201 (2004).
[6] T. Y. Chen, Y. Ji, C. L. Chien, and M. D. Stiles, Phys. Rev. Lett. **93**, 026601 (2004).
[7] S. Urazhdin, N. O. Birge, W. P. Pratt, and J. Bass, Phys. Rev. Lett. **91**, 146803 (2003).
[8] T. N. Todorov, J. Hoekstra, and A. P. Sutton, Phys. Rev. Lett. **86**, 3606 (2001).
[9] I. I. Mazin, Phys. Rev. Lett. **83**, 1427 (1999).
[10] V. P. Antropov, M. I. Katsnelson, M. van Schilfgaarde, and B. N. Harmon, Phys. Rev. Lett. **75**, 729 (1995).
[11] V. P. Antropov, M. I. Katsnelson, B. N. Harmon, M. van Schilfgaarde, and D. Kusnezov, Phys. Rev. B **54**, 1019 (1996).
[12] M. Di Ventra and S. T. Pantelides, Phys. Rev. B **61**, 16207 (2000).
[13] T. N. Todorov, J. Phys.: Condens. Matter **13**, 10125 (2001); **14**, 3049 (2002).
[14] A. R. Rocha and S. Sanvito, Phys. Rev. B **70**, 094406 (2004).
[15] A. R. Rocha, V. M. Garcia Suarez, S. W. Bailey, C. J. Lambert, J. Ferrer, and S. Sanvito, Nat. Mater. **4**, 335 (2005).
[16] R. Mota and M. D. Coutinho-Filho, Phys. Rev. B **33**, 7724 (1985).
[17] T. N. Todorov, Phys. Rev. B **54**, 5801 (1996).
[18] T. N. Todorov, J. Hoekstra, and A. P. Sutton, Philos. Mag. B **80**, 421 (2000).
[19] G. S. Rushbrooke and P. J. Wood, J. Mol. Phys. **1**, 257 (1958).
[20] J. E. Hirsch, Phys. Rev. B **56**, 11022 (1997).
[21] M. Viret, W. H. Rippard, S. Berger, M. Gabureac, F. Oh, D. Olligs, I. Petej, J. F. Gregg, C. Fermon, G. Francinet, and G. LeGoff, Phys. Rev. B **66**, 220401(R) (2002).
[22] M. R. Pufall, W. H. Rippard, S. Kaka, S. E. Rossek, T. J. Silva, J. Katine, and M. Carey, Phys. Rev. B **69**, 214409 (2004).
[23] M. Di Ventra, Y.-C. Chen, and T. N. Todorov, Phys. Rev. Lett. **92**, 176803 (2004).
[24] A. P. Sutton and T. N. Todorov, Mol. Phys. **102**, 919 (2004).